


β II-Spectrin Is Required for Synaptic Positioning during Retinal Development

Debalina Goswami-Sewell,¹  Caitlin Bagnetto,¹ Cesiah C. Gomez,¹ Joseph T. Anderson,¹ Akash Maheshwari,¹ and Elizabeth Zuniga-Sanchez^{1,2}

¹Department of Ophthalmology, Baylor College of Medicine, Houston, Texas 77030, and ²Department of Neuroscience, Baylor College of Medicine, Houston, Texas 77030

Neural circuit assembly is a multistep process where synaptic partners are often born at distinct developmental stages, and yet they must find each other and form precise synaptic connections with one another. This developmental process often relies on late-born neurons extending their processes to the appropriate layer to find and make synaptic connections to their early-born targets. The molecular mechanism responsible for the integration of late-born neurons into an emerging neural circuit remains unclear. Here, we uncovered a new role for the cytoskeletal protein β II-spectrin in properly positioning presynaptic and postsynaptic neurons to the developing synaptic layer. Loss of β II-spectrin disrupts retinal lamination, leads to synaptic connectivity defects, and results in impaired visual function in both male and female mice. Together, these findings highlight a new function of β II-spectrin in assembling neural circuits in the mouse outer retina.

Key words: neurodevelopment; retina; spectrins; synapse

Significance Statement

Neurons that assemble into a functional circuit are often integrated at different developmental time points. However, the molecular mechanism that guides the precise positioning of neuronal processes to the correct layer for synapse formation is relatively unknown. Here, we show a new role for the cytoskeletal scaffolding protein, β II-spectrin in the developing retina. β II-spectrin is required to position presynaptic and postsynaptic neurons to the nascent synaptic layer in the mouse outer retina. Loss of β II-spectrin disrupts positioning of neuronal processes, alters synaptic connectivity, and impairs visual function.

Introduction

During the development of the CNS, different neuron subtypes that assemble into a functional circuit are often born at various developmental time points (Faux et al., 2012). In order to find their respective synaptic partner, late-born neurons have the daunting task of extending their dendrites and axon into the correct layer (Faux et al., 2012). However, the molecular mechanism

of how late-born neurons know where to precisely extend their processes to form synapses with their respective targets remains poorly understood.

The mammalian retina, which is an extension of the CNS, is an excellent model to study this question. Within the retina, neurons are born at different developmental time points (Young, 1985), and yet they find their respective synaptic partner with a high degree of specificity. In the outer retina, cone photoreceptors synapse selectively to the dendrites of cone bipolar cells and the dendrites of horizontal cells, whereas rod photoreceptors synapse with the dendrites of rod bipolar cells and the axon terminal of horizontal cells (Fig. 1A). Synaptic connections are confined to the outer plexiform layer (OPL) and inner plexiform layer (IPL), whereas cell bodies of photoreceptors, interneurons, and ganglion cells are localized to the outer nuclear layer (ONL), inner nuclear layer (INL), and ganglion cell layer (GCL; see Fig. 1A). During development, cone photoreceptors first extend their axon terminal and make contacts to horizontal cells in the presumptive OPL, which is marked by the separation between the ONL and INL as shown in Figure 1B. Early OPL formation is observed starting at postnatal day (P)5 (Sarin et al., 2018; Burger et al., 2021). Bipolar neurons are born between P0 and

Received Jan. 11, 2023; revised June 16, 2023; accepted June 20, 2023.

Author contributions: D.G.-S. and E.Z.-S. designed research; D.G.-S., C.B., C.C.G., and J.T.A. performed research; D.G.-S., C.B., A.M., and E.Z.-S. analyzed data; D.G.-S. and E.Z.-S. wrote the paper; C.C.G. edited the paper.

This work was supported by National Eye Institute Grants R00EY028200 and R01EY033037 (to E.Z.-S.), an ARVO Genentech Career Development Award (E.Z.-S.), Research to Prevent Blindness (RPB) Career Development Award (E.Z.-S.), NEI vision core grant (P30EY002520) and an unrestricted grant from RPB to the Department of Ophthalmology at Baylor College of Medicine. We thank Matthew Rasband and Melanie Samuel for generously providing transgenic mouse lines, antibodies, and reagents. We also thank Ross Poché and Ching-Kang (Jason) Chen for insightful discussions throughout the development of the study. We would also like to thank Guofu Shen for help with ERG and Ralph Nichols for technical assistance with the TEM experiments.

The authors declare no competing financial interests.

Correspondence should be addressed to Elizabeth Zuniga-Sanchez at elizabeth.zuniga-sanchez@bcm.edu.

<https://doi.org/10.1523/JNEUROSCI.0063-23.2023>

Copyright © 2023 the authors

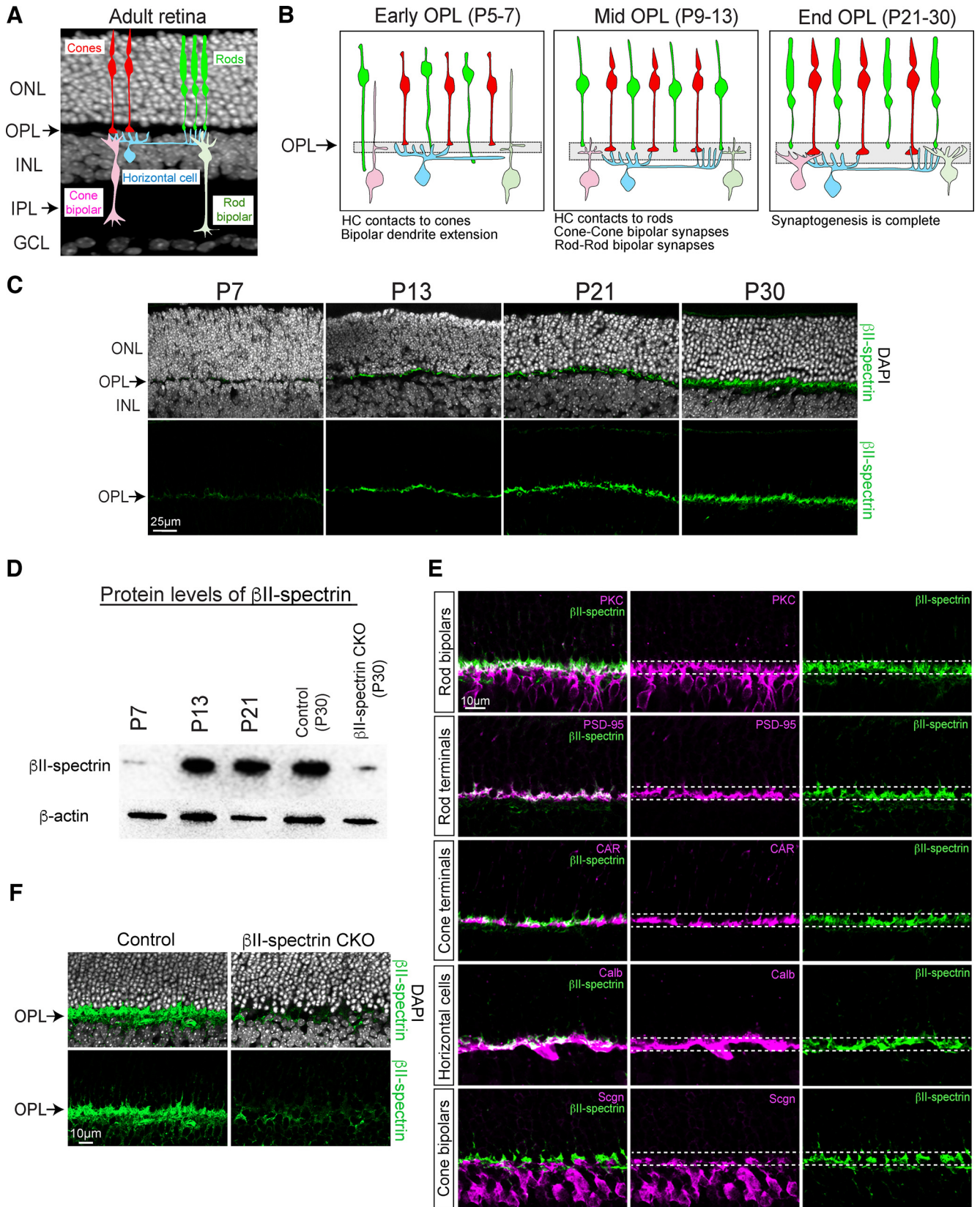


Figure 1. β II-spectrin is localized to the OPL during synaptogenesis (A–F). Schematic drawing of the adult retina. The retina is subdivided into different three nuclear layers (i.e., ONL, INL, GCL) and two synaptic layers (i.e., OPL, IPL; A). Cone photoreceptors (red) synapse to the dendrites of horizontal cells (light blue) and dendrites of cone bipolars (light red). Rod photoreceptors (green) synapse to the axon terminal of horizontal cells (light blue) and the dendrites of rod bipolars (light green; A). Development of the OPL (B). Horizontal cells (light blue) first make contacts to cones (red) in the presumptive OPL where cone bipolars (light red) and rod bipolars (light green) begin to extend their dendrites. From P9 to P13, bipolar neurons continue to extend their dendrites to the OPL and make synaptic connections to their targets. By P21, synapse formation in the retina is largely complete (B). Antibody staining of β II-spectrin (green) in wild-type retinas shows protein localization in the OPL that gradually increases from P7 to P30 (C). Nuclei is stained with DAPI (C). Western blot analysis reveals β II-spectrin protein levels increase

Table 1. List of antibodies used in this study

| Antibody name | Labeling specificity | Source | Dilution |
|---|--|---|----------|
| Mouse anti- β II-spectrin | β II-spectrin | BD Biosciences catalog #612562, RRID:AB_399853 | 1:250 |
| Rabbit anti-Cone Arrestin (CAR) | Cone photoreceptors | Millipore catalog #AB15282, RRID:AB_1163387 | 1:500 |
| Mouse monoclonal anti-Bassoon | Presynaptic photoreceptor terminals | Enzo Life Sciences catalog #VAM-PS003F, RRID:AB_1659573 | 1:500 |
| Rabbit anti-Calbindin (Calb) | Horizontal cells, amacrine cells, retinal ganglion cells | Swant catalog #CB38, RRID:AB_10000340 | 1:2000 |
| Mouse monoclonal anti-protein kinase C (PKC) | Rod bipolars | Abcam catalog #ab31, RRID:AB_303507 | 1:500 |
| Mouse polyclonal anti-PSD-95 | Photoreceptor terminals (highly expressed in rods compared with cones) | Thermo Fisher Scientific catalog #MA1-046, RRID:AB_2092361 | 1:500 |
| Rabbit polyclonal anti-metabotropic glutamate receptor 6 (mGluR6) | ON bipolar neurons | Gift from Larry Zipursky (Sarin et al., 2018) | 1:500 |
| Rabbit polyclonal anti-secretagogin (Scgn) | Cone bipolar cells | BioVendor Laboratory Medicine catalog #RD181120100, RRID:AB_2034060 | 1:1000 |
| Mouse monoclonal anti-CtBP2 | Photoreceptor Terminals | BD Biosciences catalog #612044, RRID:AB_399431 | 1:500 |
| Sheep anti-Trpm1 | Postsynaptic ON bipolar | Gift from Kirill Martemyanov (Cao et al., 2015) | 1:500 |
| Rabbit anti-Elfn1 305–320 | Rod photoreceptor terminals | Gift from Kirill Martemyanov (Cao et al., 2015) | 1:100 |

P3 (Carter-Dawson and LaVail, 1979; Young, 1985) but do not extend their dendrites into the OPL until P5 (Morgan et al., 2006). Live imaging of bipolar neurons reveal that dendrites emerge from a long neuroepithelial-like process that spans the entire retina (Morgan et al., 2006). Interestingly, only the dendrites of bipolars found within the developing OPL are stabilized and maintained whereas those that emerge in other regions are rapidly destabilized and eliminated (Morgan et al., 2006; see Fig. 1B). From P9 and P13, the long neuroepithelial-like processes from bipolar neurons disappear (Morgan et al., 2006), and synapses between photoreceptors and bipolar neurons form (Sarin et al., 2018). We refer to this time point as a midpoint of OPL formation as depicted in Figure 1B. By P21, synapse formation in the outer retina is largely complete (Sarin et al., 2018), which we refer to as the end of OPL formation in Figure 1B.

Although several key molecules have been identified that facilitate synapse formation between photoreceptors and bipolar neurons (Sato et al., 2008; Cao et al., 2015; Pourhoseini et al., 2021), to our knowledge, none have been reported to mediate the early positioning and stabilization of bipolar dendrites to the developing synaptic layer or OPL. Moreover, the functional consequence of disrupting this early developmental event remains unclear. To answer this question, we focused on the family of spectrins, as these molecules are known to mediate key signaling events by linking the cytoskeleton to the cell membrane (Bennett and Lorenzo, 2013, 2016; Lorenzo, 2020). Although spectrins play a critical role in distinct biological functions (for review, see Lorenzo, 2020), their role in synapse formation in the developing retina is unknown.

In the present study, we identified a new role for one of the members of the spectrin family, β II-spectrin in the mouse outer retina. Loss of β II-spectrin results in lamination defects whereby processes from presynaptic and postsynaptic neurons fail to be confined and maintained to the synaptic layer. This deficiency in synapse formation between photoreceptors and their synaptic partners leads to impaired retinal responses. Early developmental analysis revealed that β II-spectrin mediates the early dendrite

positioning of rod bipolars which is required for proper circuit formation. Taken together, our findings elucidate a new developmental role for β II-spectrin in assembling retinal circuits needed for proper visual function.

Materials and Methods

Mouse strains

All mouse procedures were approved by Baylor College of Medicine Institutional Animal Care and Use Committee. β II-spectrin^{flox/flox} have been described previously (Galiano et al., 2012) and were kindly provided by Matthew Rasband, Baylor College of Medicine. To remove β II-spectrin throughout the retina, β II-spectrin^{flox/flox} mice were crossed with *Chx10-Cre*^{+/-}g (Rowan and Cepko, 2004) to generate β II-spectrin conditional knock-out (CKO). β II-spectrin^{flox/flox} littermates without cre served as controls for all experiments. Wild-type retinas are from CD1 mice purchased from Charles River. Both males and females were used in all experiments.

Immunohistochemistry

Eyes were collected at various developmental time points with P0 designated as the day of birth. Whole eyes were fixed at 60 min in 4% paraformaldehyde in PBS except for mGluR6, Trpm1, CtBP2, and Elfn1 staining which were lightly fixed at room temperature for 10 min. Eye cups were dissected and sectioned at 20 μ m as previously described (Pourhoseini et al., 2021). Slides were dried overnight and washed with PBS for 10 min twice to start antibody staining. Sectioned slides were incubated with blocking buffer (10% normal goat serum, 1% BSA, 0.5% Triton X-100 in PBS) followed by primary antibodies at 4°C overnight (Table 1). Slides were washed three times with PBS for 10 min each and then incubated with secondary antibodies at 1:1000 dilution at 4°C overnight. Slides were then washed three times with PBS, stained with DAPI (1:1000), and then sealed with Vectashield (Vector Laboratories). For Elfn1 staining, retinal sections were pretreated with antigen retrieval reagents (R&D Systems, CTS013). Images were acquired on a Zeiss LSM 800 confocal microscope and analyzed using Imaris confocal software version 9.6 (Bitplane).

Histologic quantification

For quantification, images were collected from three different retinal sections from three animals per group ($n=9$) as described previously (Pourhoseini et al., 2021). β II-spectrin antibody staining was performed in all retinal sections to confirm loss of β II-spectrin in β II-spectrin CKO. All confocal images were taken from the central-periphery region of the retina. Confocal images were acquired using a Zeiss LSM 800 microscope with a 40 \times objective and then analyzed with Imaris confocal software. Quantification of presynaptic and postsynaptic marker expression was performed using the Imaris Spot feature. Puncta with a diameter of 0.6 μ m was used to detect protein expression of Bassoon, Elfn1, and Trpm1. Puncta with a diameter of 1.0 μ m was used for CtBP2 protein expression. The number of puncta in the ONL was normalized to

←

from P7 to P21 in wild-type retinas, and significantly reduced in β II-spectrin CKO compared with controls at P30 (D). β -Actin protein is shown as loading control. Co-labeling of β II-spectrin (green) with known cell type-specific markers in wild-type retinas at P30 (E). β II-spectrin protein expression (green) is significantly reduced in the OPL of β II-spectrin CKO retinas compared with controls at P30 (F). Nuclei is stained with DAPI. Scale bar shown on images.

0.01 mm² by computing the surface area of each individual retinal section. This was done by measuring the height and width of the ONL using DAPI staining. The number of puncta in the OPL per 100- μ m length was also normalized by measuring the total length of the OPL in each retinal section. Retinal layer thickness was measured in confocal sections stained with DAPI using Imaris. Statistical significance between controls and experimental groups was determined using an unpaired two-tailed Student's *t* test. All statistical analysis were performed using GraphPad Prism version 9 with *p*-values given in the text and figure legends.

RNAscope

Retinal sections were processed for *in situ* hybridization following manufacturer's instructions (Advanced Cell Diagnostics). β II-spectrin mRNA was detected using Mm-Sptbn1 (catalog #546241) probe followed by antibody staining to visualize horizontal cells (anti-Calb), rod bipolars (anti-PKC), and cone bipolars (anti-Scgn). Quantification of β II-spectrin mRNA puncta (0.8 μ m) was performed using the Imaris confocal software. A surface was created for each antibody staining and a mask was used to detect β II-spectrin mRNA puncta within individual cells. Total number of β II-spectrin mRNA puncta was analyzed in at least three retinal sections from one control and two β II-spectrin CKO animals.

Transmission electron microscopy (TEM)

Eye cups were fixed in 3% glutaraldehyde in 4°C overnight. Tissue samples were washed with 1 M sodium phosphate buffer (pH 7.3), postfixed in 1% osmium tetroxide for 1 h and dehydrated through a series of graded alcohol steps. Tissue samples were infiltrated (hardened) with acetone and polybed 812 plastic resin and embedded in plastic block molds with 100% polybed 812. Ultrathin sections (80 nm) were cut using a Leica EMUC ultra microtome. These sections were mounted on 100 mesh copper grids and stained with 2% uranyl acetate and Reynold's lead stain. Grids were visualized on a JEOL JEM 1230 electron microscope and images were captured on an AMTV600 digital camera. TEM analysis was performed on three different controls and three β II-spectrin CKO animals. Statistical significance was determined using an unpaired Student's *t* test.

Electroretinography (ERG)

Scotopic ERGs were recorded bilaterally from four control animals (*n* = 8) and five β II-spectrin CKO mice (*n* = 10) at six to eight weeks old. Mice were dark adapted overnight and anesthetized with a weight-based intraperitoneal injection solution of ketamine (46 mg/ml), xylazine (9.2 mg/ml), and acepromazine (0.77 mg/ml). We performed the ERG as described previously (Pourhoseini et al., 2021). Platinum electrodes were placed at the base of the tail and another between the ears to serve as ground and reference electrodes, respectively. Mice were moved into a Ganzfeld dome and remained in complete darkness for 5 min before initiating the experiment. Half millisecond square flashes for scotopic measurements were produced by cyan light emitting diodes of 503-nm peak wavelength. The output of the LED flashes was calibrated using a radiometer (ILT1700 International Light) with a photodiode sensor and scotopic filter that provided readout in the unit of scot cd*s/m². These were converted to the unit of photoisomerizations/rod (R*/rod) where 1 scot cd*s/m² = 581 photoisomerizations/rod/s as previously reported (Abd-El-Barr et al., 2009; Tse et al., 2015). Photopic ERG responses were elicited by using a paired-flash protocol where an initial conditioning flash (4.6×10^6 R* per M cone) saturates both rods and cones 2 s before a probe flash (1.8×10^6 R* per M cone) as described (Abd-El-Barr et al., 2009; Tse et al., 2015; Pourhoseini et al., 2021). Statistical significance was determined using the Holm–Sidak method for multiple comparisons or an unpaired Student's *t* test using the GraphPad software.

Results

β II-spectrin is localized to the developing synaptic layer

To begin to elucidate the role of β II-spectrin in the outer retina, we performed antibody staining at various developmental stages in wild-type animals. We found β II-spectrin protein localizes to

the emerging OPL where protein levels increase from P7 to P30 as seen with antibody staining in Figure 1C. These findings were confirmed by examining β II-spectrin protein levels in whole retinas by immunoblotting (Fig. 1D). Further examination reveals that β II-spectrin protein co-localizes to processes of distinct neuron types that project into the OPL, which includes dendrites of rod bipolars (anti-PKC), axon terminals of rod photoreceptors (anti-PSD-95), and processes of horizontal cells (anti-Calb; Fig. 1E). Minimal co-localization of β II-spectrin protein is seen with the axon terminals of cone photoreceptors (anti-CAR) and the dendrites of cone bipolars (anti-Scgn). Thus, these findings show that β II-spectrin is localized to the developing synaptic layer and overlaps with processes from presynaptic and postsynaptic neurons in the outer retina.

Next, we disrupted β II-spectrin function using a published floxed allele for β II-spectrin (β II-spectrin^{flox/flox}; Galiano et al., 2012) since complete germline knock-out mice of β II-spectrin are embryonically lethal (Tang et al., 2003). To conditionally remove β II-spectrin throughout the retina, we crossed β II-spectrin^{flox/flox} animals to a *Chx10-Cre*^{+tg} (Rowan and Cepko, 2004) transgenic mouse line. We refer to this cross as β II-spectrin CKO. Immunoblotting showed a reduction but not complete absence of β II-spectrin protein in whole retinas of β II-spectrin CKO compared with controls (Fig. 1D), and antibody staining also showed partial knock-down of β II-spectrin within the OPL (Fig. 1F). These findings are consistent with work from our lab (Pourhoseini et al., 2021) as well as others (Lefebvre et al., 2008) showing mosaic expression and partial knock-down with the *Chx10-Cre*^{+tg} transgenic mouse line.

We then addressed cell type-specific expression of β II-spectrin by performing *in situ* hybridization in both control and β II-spectrin CKO animals during synapse formation (i.e., P13). We found β II-spectrin mRNA is detected throughout the retina with the highest level found within the INL (Fig. 2A). This finding is consistent with published single cell sequencing data showing high levels of β II-spectrin within bipolar neurons compared with other β -spectrin family members (Shekhar et al., 2016). Moreover, a comparison between control and β II-spectrin CKO revealed an overall reduction of β II-spectrin mRNA throughout the retina as shown in Figure 2A. To confirm this observation, we quantified the total number of β II-spectrin mRNA puncta (0.8 μ m in size) in the different nuclear layers. For our analysis, we focused on the top-half of the INL (referred to as top-INL) as this is where the cell bodies of postsynaptic neurons to photoreceptors reside. We found a significant reduction of β II-spectrin mRNA in the ONL (control: 130.7 ± 63.2 puncta; β II-spectrin CKO: 45.3 ± 18.8 puncta) and the top-INL (control: 800 ± 160.7 puncta; β II-spectrin CKO: 359.6 ± 78.5 puncta), but not within the GCL (control: 901.4 ± 345.6 ; β II-spectrin CKO: 926.7 ± 117.6). As β II-spectrin mRNA levels are the highest within the INL in controls, we further examined cell type-specific expression by co-staining with known markers of rod bipolars (anti-PKC), cone bipolars (anti-Scgn), and horizontal cells (anti-Calb; see Fig. 2B). Our data revealed a significant reduction in the number of β II-spectrin mRNA puncta within rod bipolars (controls: 3.1 ± 1.9 puncta per cell from 47 rod bipolars; β II-spectrin CKO-1: 1.5 ± 1.2 puncta per cell from 34 rod bipolars; β II-spectrin CKO-2: 1.7 ± 1.2 puncta per cell from 49 rod bipolars). Similar to rod bipolars, we also noticed a significant decrease of β II-spectrin mRNA expression within cone bipolars (controls: 7.1 ± 2.5 puncta per cell from 50 cone bipolars; β II-spectrin CKO-1: 3.8 ± 1.8 puncta per cell from 42 cone bipolars; β II-spectrin CKO-2: 3.4 ± 1.8 puncta per cell from 49 cone bipolars). However,

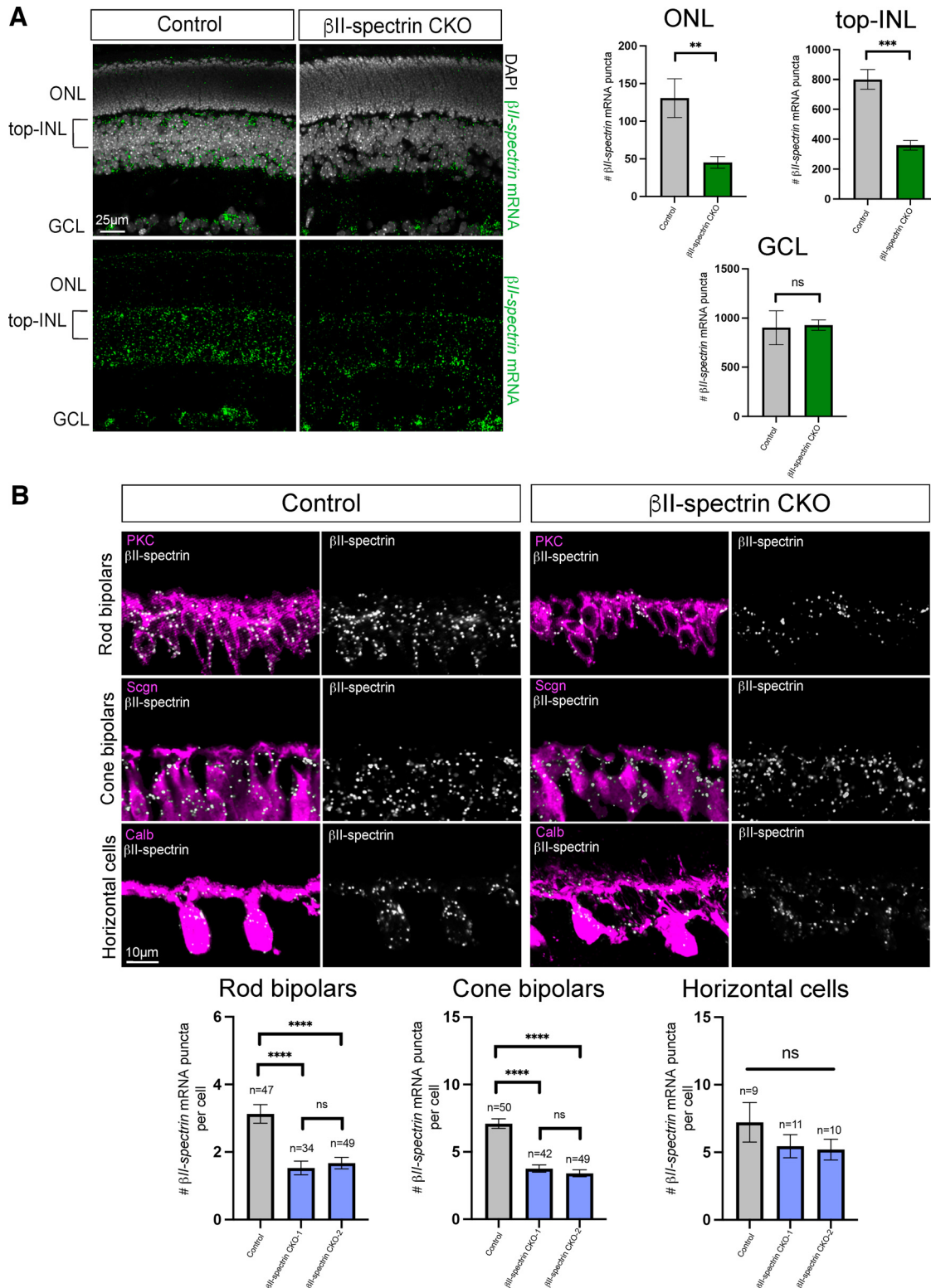


Figure 2. β II-spectrin mRNA is highly expressed in the INL and significantly reduced in rod bipolars and cone bipolars of β II-spectrin CKO animals (**A, B**). β II-spectrin mRNA (green) was detected via *in situ* hybridization using RNAscope technology at P13. A significant reduction of β II-spectrin mRNA was observed in the ONL and INL but not the GCL in β II-spectrin CKO compared with controls (**A**). Quantification of the total number of β II-spectrin mRNA puncta in each nuclear layer (i.e., ONL, INL, GCL) is shown in **A**. DAPI staining was used to visualize the distinct nuclear layers. The number of puncta was normalized to an area of 0.01mm² by computing the surface area of each individual retinal section. Antibody staining was performed immediately after *in situ* hybridization to detect β II-spectrin mRNA within individual cell types at P13 (**B**). Quantification of β II-spectrin mRNA puncta (0.8 μ m in size) per cell is shown in **B** with n representing the total number of cells analyzed per animal. β II-spectrin mRNA (white) is highly expressed in rod bipolars (anti-PKC, magenta) in controls and significantly reduced in β II-spectrin CKO. Similarly, cone bipolars (anti-Scgn, magenta) also express β II-spectrin mRNA in controls and show a reduction in the number of puncta in β II-spectrin CKO. However, β II-spectrin mRNA levels in horizontal cells (anti-Calb, magenta) are not statistically different between controls and β II-spectrin CKO. Data are represented as mean values \pm SEM. Statistical significance determined by an unpaired two-tailed Student's *t* test. ns $p > 0.05$, ** $p < 0.01$, *** $p = 0.0001$, **** $p < 0.0001$. Scale bar shown for each figure.

there was no significant difference of β II-spectrin mRNA puncta within horizontal cells (controls: 7.2 ± 4.4 puncta per cell from nine horizontal cells; β II-spectrin CKO-1: 5.5 ± 2.8 puncta per cell from 11 horizontal cells; β II-spectrin CKO-2: 5.2 ± 2.4 puncta per cell from 10 horizontal cells). These findings demonstrate that β II-spectrin is widely expressed throughout the retina, with the highest level of expression found within the INL. Furthermore, our β II-spectrin CKO transgenic mouse line preferentially disrupts expression of β II-spectrin within the ONL and INL, with a significant reduction of β II-spectrin mRNA in rod bipolars and cone bipolars.

Disruption of β II-spectrin results in lamination defects in the outer retina

We then examined adult retinas from β II-spectrin CKO and controls for morphologic and synaptic defects. Nuclei staining with DAPI at P30 revealed no gross morphologic defects in the overall retinal structure of β II-spectrin CKO compared with controls (Fig. 3A). Measurements of the layer thickness of the ONL and INL revealed no significant difference between controls and β II-spectrin CKO (Fig. 3A). However, the OPL was significantly thinner by 82% in β II-spectrin CKO compared with controls with several displaced nuclei found within the synaptic layer as depicted by yellow arrows in Figure 3A. As loss of β II-spectrin does not disrupt the overall structure of the retina, we then used several known markers of presynaptic and postsynaptic neurons to assess for synaptic defects. By P30, synapse formation is largely complete in the outer retina and neuronal processes from presynaptic and postsynaptic neurons are confined to the OPL as seen in controls in Figure 3B. We found that disruption of β II-spectrin leads to numerous processes (or sprouts) of horizontal cells extending beyond the OPL into the ONL (Fig. 3B). Controls displayed an average of 0.07 ± 0.12 sprouts per 100- μ m length of OPL, whereas β II-spectrin CKO showed 7.70 ± 3.28 sprouts per 100- μ m length of OPL (Fig. 3B). Similarly, the dendrites of rod bipolars also failed to be confined to the OPL and instead misprojected into the ONL. The average number of rod bipolar sprouts in β II-spectrin CKO was 5.83 ± 3.21 per 100- μ m length of OPL, whereas controls displayed no detectable sprouts (Fig. 3B). However, very few sprouts from the dendrites of cone bipolars were observed in β II-spectrin CKO (1.90 ± 0.67 sprouts per 100- μ m length of OPL) as shown in Figure 4A,C. These results indicate β II-spectrin is required for positioning and maintaining processes from postsynaptic neurons such as horizontal cells and rod bipolars but not cone bipolars in the OPL. Moreover, we also counted the total number of horizontal cells and rod bipolars in retinal sections of controls and β II-spectrin CKO and found no significant difference between the two groups (Fig. 3B). These data suggest that the sprouting phenotype of horizontal cells and rod bipolars seen in β II-spectrin CKO cannot be simply explained because of cell death.

We next addressed the role of β II-spectrin on presynaptic neurons by examining the position of photoreceptor terminals using antibodies against Cone Arrestin (CAR) for cone terminals and PSD-95 for rod terminals. PSD-95 is expressed in both rod and cone terminals, however higher levels of protein expression are found in rods compared with cones (Sarin et al., 2018). We found the overall number of cone terminals in the OPL was not statistically different between β II-spectrin CKO (10.51 ± 1.51 cone terminals) and controls (9.87 ± 0.53 cone terminals) at P30 (see Fig. 4B,C). However, examination of rod terminals with PSD-95 staining revealed a shift in protein localization where expression becomes more diffuse (i.e., less in the OPL and ectopic puncta-like expression in the ONL; Figs. 3C, 4A). Ectopic

PSD-95 protein expression in the ONL has been associated with rod retraction and loss of synaptic connectivity (Samuel et al., 2014). Thus, we set out to further examine photoreceptor synapses in β II-spectrin CKO using available antibodies.

β II-spectrin is required for rod synaptic connectivity and retinal function

We examined protein localization of presynaptic markers such as Bassoon (Bsn) and CtBP2 that are both expressed in rod and cone terminals (Pourhoseini et al., 2021). We found Bsn and CtBP2 protein expression is reduced in the OPL and ectopically expressed in the ONL with disruption of β II-spectrin (Figs. 3C, 4B). Bsn and CtBP2 protein form a puncta-like structure that is roughly 0.6 and 1.0 μ m in diameter, respectively. The total number of Bsn and CtBP2 puncta were quantified using Imaris software in both controls and β II-spectrin CKO at P30 (Fig. 3E). Nearly 92% of total Bsn puncta were localized to the OPL in controls whereas 44% is found in the OPL in β II-spectrin CKO. A similar distribution was also observed with CtBP2 where 88% of puncta is in the OPL of controls and 7% in β II-spectrin CKO (Fig. 3E). However, the number of Bsn puncta within cone terminals was not statistically different between controls and β II-spectrin CKO (Fig. 4C). Next, we examined the expression of Elnf1 which is expressed in rod photoreceptors and required for selective wiring of rods to their synaptic partners (Cao et al., 2015). Interestingly, we found Elnf1 protein expression mostly absent in β II-spectrin CKO compared with controls (Fig. 3C,E). Similarly, postsynaptic protein expression of Trpm1 and mGluR6 are also reduced because of loss of β II-spectrin (Fig. 3C,D) with quantification of Trpm1 puncta shown in Figure 3E. Together, these results demonstrate β II-spectrin is required for proper localization and expression of synaptic proteins implicated in rod synaptic connectivity.

To further address whether changes in synaptic protein expression translate to rod connectivity defects, we performed transmission electron microscopy (TEM) to examine the rod synaptic structure in both controls and β II-spectrin CKO at P30. Consistent with our synaptic protein findings, we found an overall reduction in the number of rod terminals localized to the OPL with several mispositioned in the ONL (Fig. 5A,B). For controls, we analyzed a total of 56 TEM sections from three different animals and observed 1555 rod terminals in the OPL. For β II-spectrin CKO, we analyzed 63 TEM sections from three mice and found only 296 rod terminals in the OPL (Fig. 5B). Moreover, we classified rod terminals into four categories: (1) empty, no visible processes; (2) monads, only one invaginating process; (3) dyads, two invaginating processes; (4) triads, two invaginating processes from horizontal cells and one from an ON bipolar dendrite. Our analysis revealed an increase in the number of empty rod terminals and a decrease in the number of triads in the OPL of β II-spectrin CKO compared with controls (Fig. 5B). These data suggest β II-spectrin is required for positioning rod terminals to the OPL.

We next asked whether the rod synaptic defects observed in β II-spectrin CKO impairs retinal function by performing *in vivo* full-field electroretinograms (ERG) in dark-adapted mice. Mice were exposed to flashes of light of varying intensities to measure rod-driven responses or scotopic ERG. Cone-driven responses or photopic ERG were elicited using a paired-flash protocol as described previously (Abd-El-Barr et al., 2009; Pourhoseini et al., 2021). Individual ERG traces of controls (black line) and β II-spectrin CKO (blue line) at different stimulus intensities are shown in Figure 5C. The a-wave

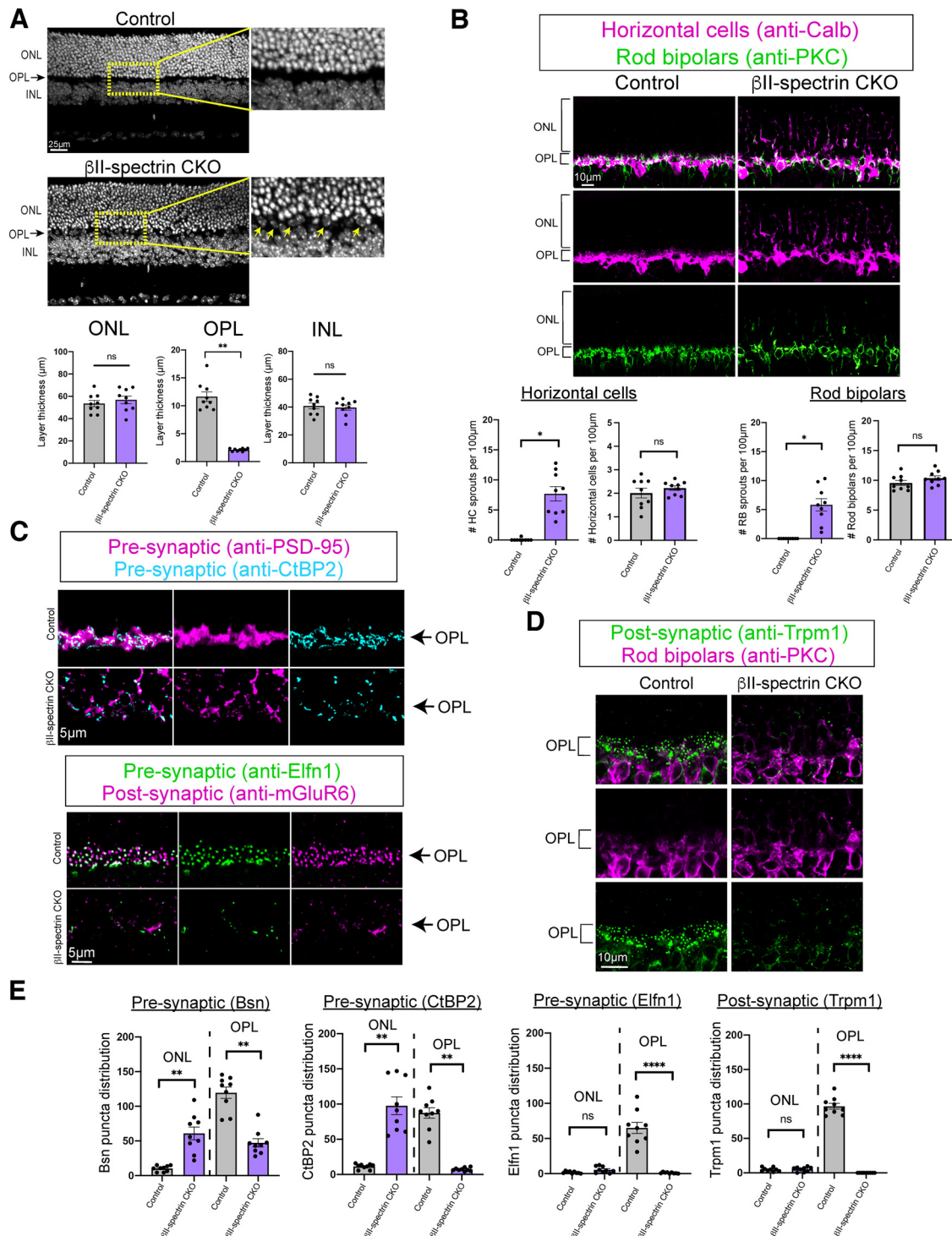


Figure 3. Loss of β II-spectrin results in lamination defects in the outer retina (**A–E**). Retinal sections of control and β II-spectrin CKO stained with DAPI reveal no gross morphologic defects (**A**). Close examination of the OPL show several displaced nuclei in β II-spectrin CKO as depicted by the yellow arrows. Insets are zoomed images of yellow dotted boxed region. Measurements of the layer thickness show no significant difference between the ONL and INL but a significant decrease in the OPL of β II-spectrin CKO compared with controls (**A**). Disruption of β II-spectrin results in lamination defects where processes from horizontal cells (anti-Calb, magenta) and dendrites of rod bipolar cells (anti-PKC, green) failed to be confined to the OPL and instead sprout into the ONL (**B**). Quantification of the total number of sprouts observed in controls and β II-spectrin CKO (**B**). Total cell counts of horizontal cells and rod bipolar cells are shown in **B**. Expression and localization of presynaptic PSD-95 (magenta) and CtBP2 (cyan) are also affected in β II-spectrin CKO compared with controls (**C**). Loss of presynaptic Efn1 (green) and postsynaptic mGluR6 (magenta) protein expression is seen in the OPL because of disruption of β II-spectrin (**C**). Postsynaptic Trpm1 (green) forms a puncta-like structure along the dendrites of rod bipolar cells in controls but is significantly reduced in β II-spectrin CKO (**D**). Quantification and localization of presynaptic and postsynaptic markers (i.e., Bsn, CtBP2, Efn1, Trpm1) at P30 (**E**). The number of Bassoon puncta ($\sim 0.6 \mu$ m in size) and CtBP2 (1.0μ m in size) is significantly reduced in the OPL and increased in the ONL because of loss of β II-spectrin. Presynaptic Efn1 puncta ($\sim 0.6 \mu$ m in size) and postsynaptic Trpm1 puncta ($\sim 0.6 \mu$ m in size) are significantly reduced in the OPL in β II-spectrin CKO compared with controls. Images are shown as confocal sections. Data are represented as mean values \pm SEM. Statistical significance determined by an unpaired two-tailed Student's *t* test. ns $p > 0.05$, * $p < 0.05$, ** $p < 0.01$, **** $p < 0.0001$. Scale bar shown for each figure.

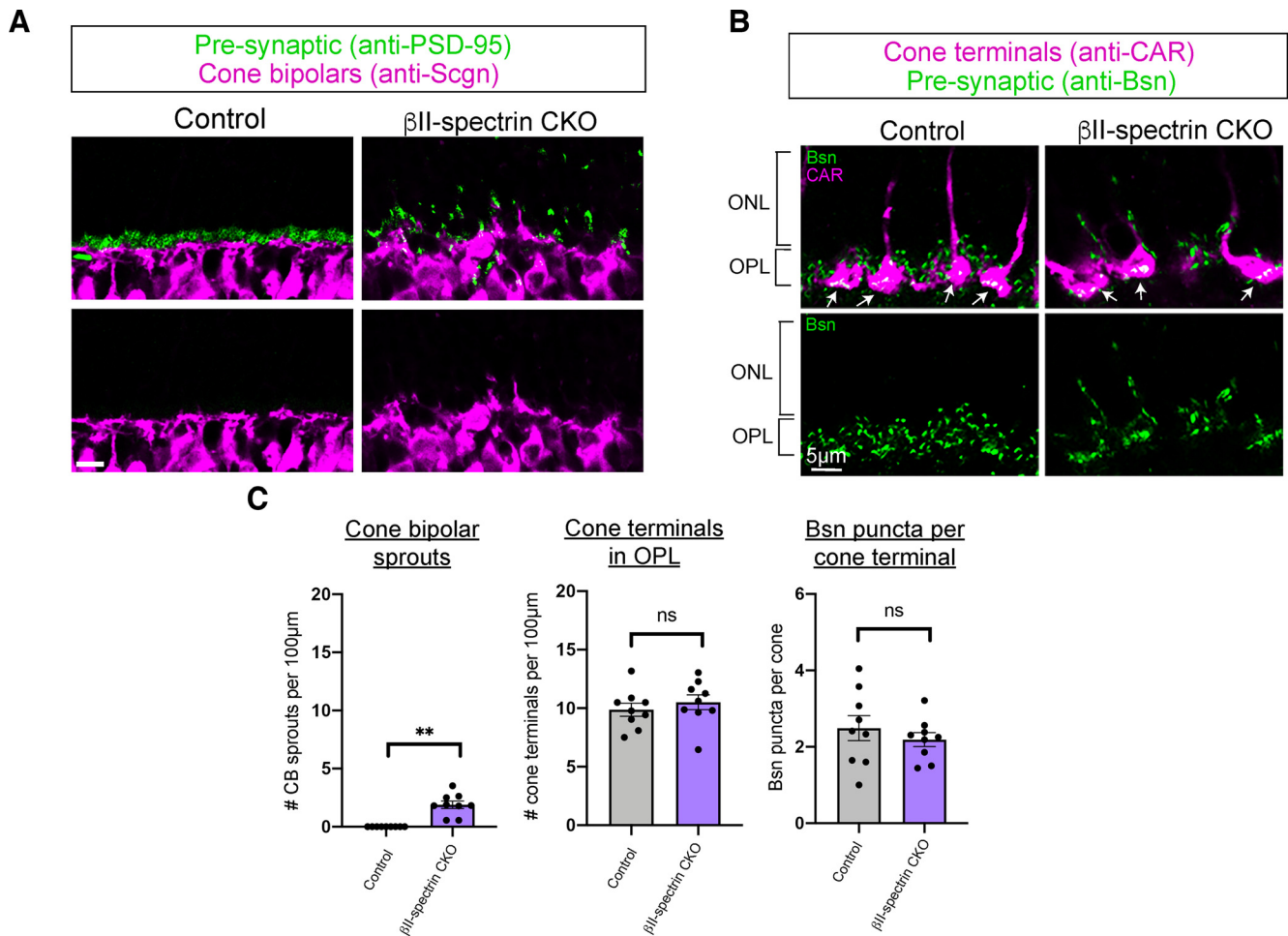


Figure 4. Minimal defects in the cone pathway because of loss of β II-spectrin (**A–C**). Presynaptic PSD-95 protein (green) is enriched in rod terminals as seen in controls (**A**). Redistribution of PSD-95 protein expression is observed in β II-spectrin CKO where there is loss in the OPL and ectopic expression in the ONL (**A**). Dendrites of cone bipolars (magenta, anti-Scgn) show minimal number of sprouts in β II-spectrin CKO compared with controls (**A**). Bassoon (anti-Bsn, green) is localized to the OPL in controls but reduced in the OPL and ectopically expressed in the ONL of β II-spectrin CKO animals at P30 (**B**). Cone terminals (anti-CAR, magenta) are normally positioned in the OPL and express Bassoon in both controls and β II-spectrin CKO as depicted by white arrows (**B**). Quantification of the total number of cone bipolar sprouts, number of cone terminals in OPL, and number of presynaptic Bassoon (Bsn) puncta in cone terminals (**C**). The number of cone terminals in the OPL and the number of Bsn puncta were not statistically different ($p > 0.05$) between controls and β II-spectrin CKO. Statistical significance determined by an unpaired two-tailed Student's t test. ns $p > 0.05$, ** $p < 0.005$. Scale bar, 10 μ m.

represents photoreceptor responses whereas the b-wave is the downstream synaptic response from both outer and inner retinal neurons (Abd-El-Barr et al., 2009). Our results show an overall reduction in b-wave responses but not a-wave responses under scotopic conditions because of disruption of β II-spectrin. To confirm these findings, we plotted b-wave responses fitted with the Naka-Rushton equation and calculated the maximum rod-driven b-wave response (i.e., Bmax). We found controls had a Bmax value of 540 μ V (black dotted line) whereas β II-spectrin CKO had a Bmax of 197 μ V (blue dotted line) as shown in Figure 5D. Although scotopic b-wave responses are significantly reduced in β II-spectrin CKO compared with controls, the time-to-peak or implicit time is not affected (Fig. 5F). However, rod-driven or scotopic a-wave responses in dark-adapted mice were not statistically different between controls and β II-spectrin CKO at low flashes of light but were significant at higher flashes of light when both rods and cones are activated (Fig. 5E). To further investigate cone-driven or photopic responses, we isolated the cone a-wave and b-wave and found no statistical difference between controls and β II-spectrin CKO using an unpaired Student's t test ($p < 0.05$) as shown in Figure 5G.

Together, these data show impaired rod-driven downstream responses or scotopic b-wave in β II-spectrin CKO compared with controls, which support the synaptic connectivity defects observed with loss of β II-spectrin.

Temporal requirements of β II-spectrin in the outer retina

We then asked when is β II-spectrin required for synaptic connectivity in the outer retina. To answer this question, we performed a developmental analysis at early stages of synaptogenesis (i.e., P9, P11, P13) in β II-spectrin CKO animals. We focused our analysis on rod bipolars and horizontal cells as these retinal neurons show significant lamination defects at adult stages (Fig. 3B). We found that by P9 the dendrites of rod bipolars extend into the OPL and form one continuous layer as seen in controls (Fig. 6A). However, we observed gaps or areas where the dendrites of rod bipolars failed to extend in the OPL (yellow arrow) and instead sprout into the ONL (white arrows) because of loss of β II-spectrin (Fig. 6A). The total number of rod bipolar sprouts continued to increase from P9 to P13 as shown in Figure 6B. Interestingly, we did not observe gaps or sprouts of processes from horizontal cells at P9 (Fig. 6A). However, the number of horizontal cell sprouts did

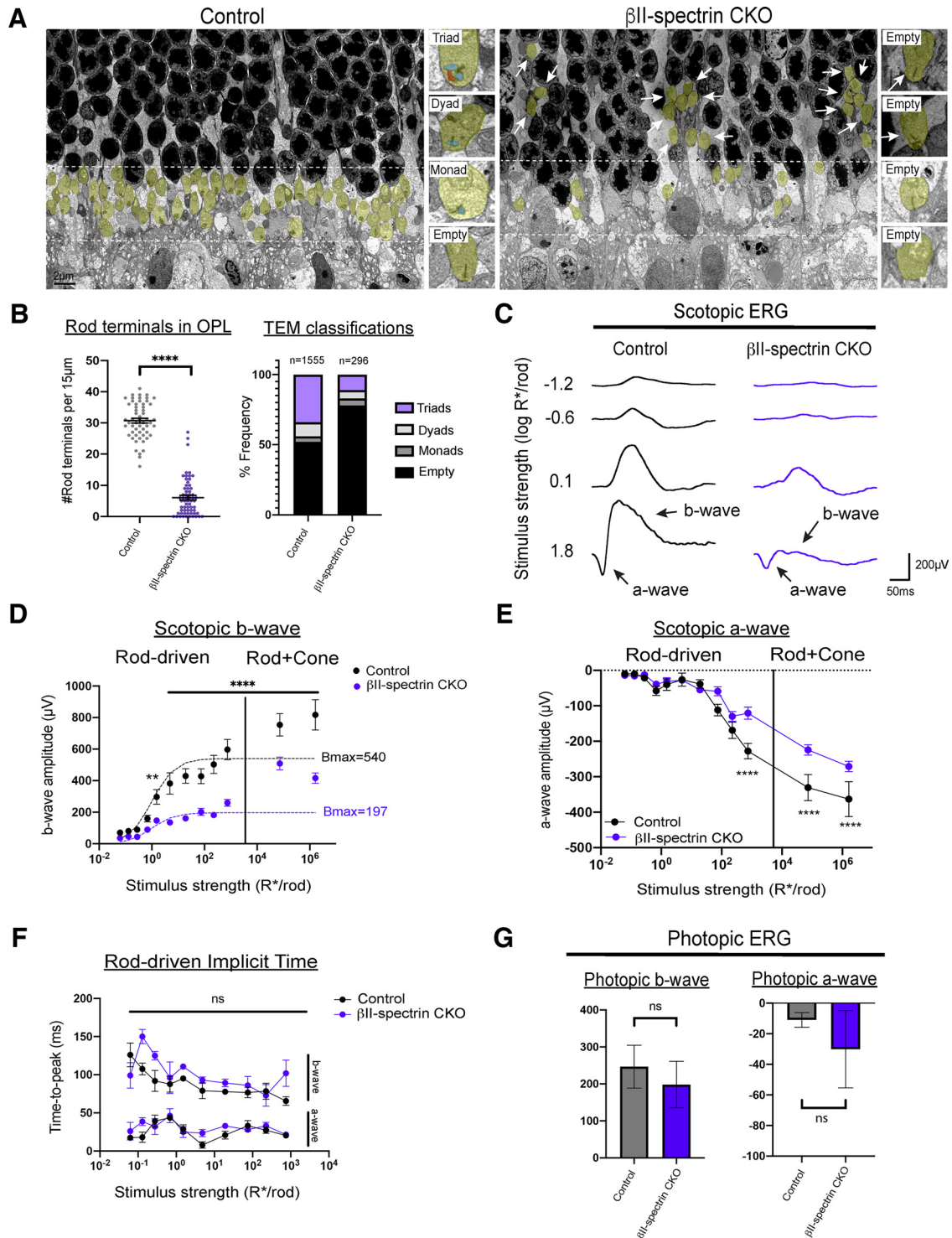


Figure 5. Synaptic defects and abnormal retinal responses in β II-spectrin CKO (**A–G**). Transmission electron microscopy (TEM) reveals rod terminals (yellow) are not localized to the OPL (white dotted lines) but mispositioned in the ONL (white arrows) because of loss of β II-spectrin (**A**). The number of rod terminals in the OPL were counted in both controls and β II-spectrin CKO (**B**). Data are represented as mean values \pm SEM. Statistical significance determined by an unpaired two-tailed Student's *t* test. *****p* < 0.0001. Rod terminals were classified as either triad, dyad, monad, or empty (**B**). A total of 1555 rod terminals were found in the OPL and analyzed in controls; however, only 296 rod terminals were observed in the OPL of β II-spectrin CKO (**B**). The frequency of triads, dyads, monads, and empty in controls and β II-spectrin CKO revealed an increase in the number of empty rod terminals because of disruption of β II-spectrin (**B**). Individual electroretinogram (ERG) traces from controls (black line) and β II-spectrin CKO (blue line) are shown at different scotopic or rod-driven stimulus intensities (**C**). Scotopic b-wave amplitudes are significantly reduced in β II-spectrin CKO (blue line, *n* = 10 from five mice) compared with controls (black line, *n* = 8 from four mice; **D**). Data points within the rod operative range are fitted with a hyperbolic saturating curve using the Naka-Rushton equation. Stimulus response plot of scotopic a-wave amplitudes of dark-adapted controls (black line, *n* = 8 from four mice) and β II-spectrin CKO (blue line, *n* = 10 from five mice; **E**). Statistical significance determined by Holm–Sidak method for multiple comparisons in **D**, **E** and **F**. ns *p* > 0.05, ***p* < 0.005, *****p* < 0.0001. Rod-driven implicit times are shown for controls (black line, *n* = 8 from four mice) and β II-spectrin CKO (blue line, *n* = 10 from five mice; **F**). Isolated amplitudes of the cone b-wave and a-wave using the paired flash method (**G**). Data represented as mean values \pm SD. Statistical significance determined by an unpaired two-tailed Student's *t* test (ns *p* > 0.05).

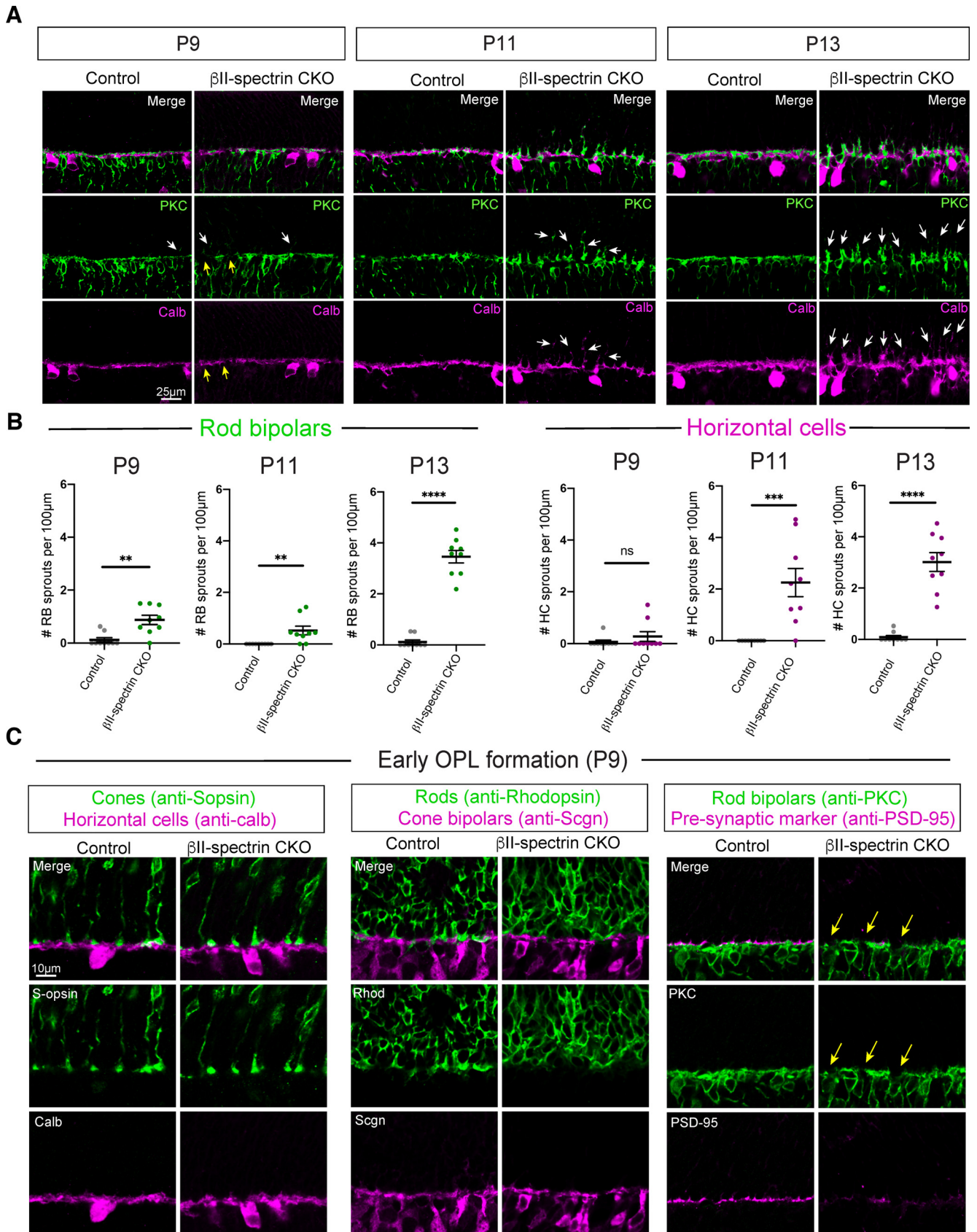


Figure 6. Developmental analysis of β II-spectrin CKO (A–C). At P9, dendrites of rod bipolars (green, anti-PKC) and processes from horizontal cells (magenta, anti-calb) form one continuous laminated structure in controls (A). However, several mispositioned dendrites of rod bipolars such as gaps (yellow arrows) and sprouts (white arrows) are observed in β II-spectrin CKO. Mispositioned processes or sprouts from horizontal cells (white arrows) are not detected until P11 in β II-spectrin CKO and continue to P13 (A). Quantification of the total number of rod bipolar and horizontal cell sprouts per 100- μ m length of OPL across the different time points (B). Few sprouts are observed in controls compared with β II-spectrin CKO from P9 to P13 (A, B). Statistical significance determined by an unpaired two-tailed Student’s *t* test. ns $p > 0.05$, ** $p < 0.005$, *** $p < 0.001$, **** $p < 0.0001$. Processes from other presynaptic and postsynaptic

increase from P11 to P13 in β II-spectrin CKO compared with controls (Fig. 6A,B). These findings suggest that the improper positioning of the dendrites of rod bipolars at early stages (i.e., P9) may lead to the subsequent lamination defects seen in horizontal cells. We also examined the position of cone terminals (anti-S-opsin), dendrites of cone bipolars (anti-Scgn), and rods (anti-Rhodopsin) at P9 (Fig. 6C). Although we do see gaps or defects in dendrite extension of rod bipolars (anti-PKC) and loss of presynaptic protein expression (anti-PSD-95) in β II-spectrin CKO, we do not observe defects in the positioning of other retinal cell types (Fig. 6C). These findings further support the model that β II-spectrin is required early on to position the dendrites of rod bipolars to the emerging OPL.

Discussion

In the present study, we uncovered a new role of β II-spectrin in assembling neural circuits in the mouse outer retina. We found β II-spectrin positions and maintains the processes of presynaptic and postsynaptic neurons to the developing synaptic layer or OPL. Loss of β II-spectrin results in lamination defects where processes fail to be confined to the OPL resulting in impaired synaptic connectivity and abnormal retinal responses. These findings highlight a new key player in neural circuit formation required for normal visual function.

Spectrins in the developing nervous system

Spectrins play an essential role in the CNS. They are known to indirectly bind to cell adhesion molecules, receptors, ion channels, and other scaffolding proteins (Bennett and Lorenzo, 2013, 2016; Lorenzo, 2020). Early studies have shown spectrins play an important role in synaptic connectivity of the *Drosophila* neuromuscular junction (Pielage et al., 2006); however, their role in the developing mammalian nervous system is unclear.

Individuals with mutations in SPTBN2, the gene encoding for β III-spectrin has been associated with spinocerebellar ataxia type 5 in humans (Ikeda et al., 2006). Mice with loss of β III-spectrin display defects in dendrite morphology of Purkinje cells and cerebellar degeneration (Perkins et al., 2010). Human mutations in SPTBN1, gene encoding for β II-spectrin display mild to severe intellectual disabilities, language and motor deficits, seizures, and behavioral abnormalities (Cousin et al., 2021). Similarly, mice that lack β II-spectrin in neural progenitors display motor coordination deficits, multiple seizures, reduced long-range axonal connectivity, and early postnatal lethality (Lorenzo et al., 2019). The widespread neurologic defects observed with loss of spectrins suggest that they have distinct functions in setting up different neural circuits.

Our findings uncovered a new key molecule that is required for the early positioning and stabilization of late-born neurons to the emerging synaptic layer. Although dendrite extension of bipolar neurons into the OPL has been well documented (Morgan et al., 2006), the significance of this process on synapse formation had been relatively unknown.

We found loss of β II-spectrin disrupts the normal positioning of the dendrites of rod bipolar at early stages and this leads to defects in synaptic connectivity and impaired retinal responses in the adult. Throughout the CNS, neurons are integrated into a nascent neural circuit at various stages during development (Faux et al., 2012). Defects in neuron migration, targeting, and connectivity are often linked to neurodevelopmental disorders such as intellectual disability, epilepsy, and autism spectrum disorder (Bozzi et al., 2012; Moon and Wynshaw-Boris, 2013; Pan et al., 2019). However, disseminating the mechanisms involved in neural circuit assembly has remained challenging. Several key molecules including spectrins are known to play multiple roles throughout development (Lorenzo, 2020). Spectrins are known to mediate early roles in neurodevelopment such as cell migration, neuron morphology, and axon outgrowth (Lorenzo et al., 2019; Lorenzo, 2020; Cousin et al., 2021). Thus, the retina is an excellent model where we can take advantage of the different experimental approaches that can tease apart the early and later temporal requirements of spectrins to elucidate their multiple functions.

β II-spectrin function in the outer retina

The mouse retina is an excellent system to uncover new developmental mechanisms of neural circuit assembly. The various transgenic mouse lines and tools that are readily available in the retina allows us to disrupt gene function in both a cell-type and temporal manner. Germline knock-outs of β II-spectrin are embryonically lethal (Tang et al., 2003). Thus, we were able to bypass the early requirements of β II-spectrin using retinal-specific cre lines that turns on at later stages in development (Rowan and Cepko, 2004). This allowed us to uncover a new role of β II-spectrin in assembling neural circuits that occurs at later developmental time points.

Our developmental analysis showed that β II-spectrin is required early on to position the dendrites of rod bipolars to the emerging synaptic layer. As lamination defects are often seen in mouse mutants with synaptic connectivity defects (Dick et al., 2003; Soto et al., 2013; Ribic et al., 2014), this raises the question whether β II-spectrin is directly involved in remodeling the cytoskeleton or indirectly mediates synapse formation through recruitment of cell adhesion molecules. For instance, recent studies show that β II-spectrin acts on the axon terminal of cultured neurons, where loss of β II-spectrin disrupts axonal transport and inhibits axon growth (Lorenzo et al., 2019). β II-spectrin has been shown to interact with membrane lipids and this is required for dynein/dynactin axonal transport (Muresan et al., 2001). Mutations in β II-spectrin that disrupt binding with membrane lipids leads to defects in axonal transport and growth (Hyvönen et al., 1995). These data raise the possibility that β II-spectrin in rod bipolars may mediate the direct outgrowth of the dendrites into the developing synaptic layer by interacting with membrane lipids to mediate dendritic transport and growth. Another possibility is that β II-spectrin may act indirectly on synapse formation by recruiting and maintaining cell adhesion molecules to the cell surface. Studies in myelinated axons demonstrate spectrins indirectly bind to cell adhesion molecules to mediate the precise positioning of the nodes of Ranvier (Galiano et al., 2012; Rasband and Peles, 2021). One of the known binding partners of spectrins is the L1-family cell adhesion molecule, Neurofascin (Eshed et al., 2005; Ho et al., 2014; Rasband and Peles, 2021). Previous work from our lab showed Neurofascin is expressed in the developing synaptic layer and required for proper connectivity between rod photoreceptors and their

←

neurons are normally positioned to the nascent OPL at P9 (C). Cone terminals (green, anti-S-opsin) and processes from horizontal cells (magenta, anti-calb) are localized to the developing OPL in both controls and β II-spectrin CKO. Rods (green, anti-Rhodopsin) and dendrites of cone bipolars (magenta, anti-Scgn) are largely confined to the OPL at P9 in controls and β II-spectrin CKO. Dendrites of rod bipolars (green, anti-PKC) begin to display gaps and loss of presynaptic protein expression (magenta, anti-PSD-95) as depicted by yellow arrows because of loss of β II-spectrin. Scale bar shown on figures.

synaptic targets (Pourhoseini et al., 2021). However, loss of Neurofascin does result in lamination defects as those seen with loss of β II-spectrin suggesting that there may be other binding partners in the outer retina. Future studies are needed to identify the downstream mechanism of how β II-spectrin mediates synapse formation in the developing retina.

Site of β II-spectrin function in the outer retina

Our findings revealed β II-spectrin is widely expressed throughout the retina in several cell types including photoreceptors, bipolar neurons, and horizontal cells. We also found that β II-spectrin mRNA levels is reduced in multiple retinal neuron types in β II-spectrin CKO compared with controls. This raises the question of which β II-spectrin-expressing cell mediates proper positioning of synapses in the mouse retina. The challenge to tackle this question is that the β II-spectrin CKO phenotype could be because of a compilation of different functions where β II-spectrin is required in distinct cell types at precise time points during development. This would mean that single cell type-specific knock-outs of β II-spectrin may not yield a phenotype, and only knock-down in multiple cell types such as in the case of β II-spectrin CKO will produce synaptic defects. Another obstacle is that several of the transgenic mouse lines and available tools are not very efficient in knocking out genes at early developmental stages. For example, the rod-specific cre mouse line or *Rhoicre* begins to express cre starting at P7 and cre-mediated excision is not complete until P18 (Li et al., 2005). This poses a problem as we observe high levels of β II-spectrin protein expression from P7 to P13, which may be too late to disrupt β II-spectrin in rod photoreceptors. Similarly, mouse lines to target bipolar neurons such as *Grm6-cre*, *Cck-cre*, and *Kcng4-cre* show very weak expression at early developmental stages (Hoon et al., 2015; Shekhar et al., 2016) with *Cck-cre* and *Kcng4-cre* also being expressed in other retinal neuron types (Martersteck et al., 2017). Moreover, some of the tools to knock-down gene function especially within bipolar neurons are not very efficient. For instance, CRISPR-based retinal electroporation techniques is a robust method of knocking down gene in the mouse retina (Sarin et al., 2018). However, one of the limitations of this approach is that very few bipolar neurons are transfected with this method which may lead to incomplete knock-down of β II-spectrin and no phenotype. Thus, currently there are no robust and efficient methods that can be used to disseminate the cell-type and temporal requirements of β II-spectrin function within the retina.

Assembling complex neural circuits during development

Recent work in the retina begin to shed light into the complexity of assembling neural circuits. Over the last decade, several new molecules have been identified to mediate different aspects of synapse formation and maintenance in the outer retina (Hoon et al., 2014; Zhang et al., 2017; Burger et al., 2021). However, how these molecules work together during development to mediate the precise connectivity of synaptic partners remains unclear. Studies using different mutant mouse lines begin to illustrate differences in synaptic phenotypes when different molecules are disrupted during synaptogenesis. These phenotypes can be largely grouped into three main classes: (1) defects in both retinal lamination and synaptic connectivity, (2) defects in retinal lamination only, and (3) defects in synaptic connectivity only (Zhang et al., 2017; Burger et al., 2021). Although our findings revealed β II-spectrin leads to defects in both retinal lamination and synaptic connectivity, the changes in

protein expression reflect a later stage in synapse formation. Both Bassoon and Elnf1 are localized to the axon terminal of rod photoreceptors and loss of protein expression in mutant mice disrupts rod synaptic connectivity (Dick et al., 2003; Cao et al., 2015). Our data revealed loss of β II-spectrin leads to ectopic expression of Bassoon and CtBP2 but absence of Elnf1 and PSD-95. Previous work has shown Bassoon expression appears at early stages in synapse development (Sarin et al., 2018), whereas Elnf1 turns on at later stages and expression is reinforced after synapse formation (Cao et al., 2015). These data show how different synaptic proteins may be required at different stages during synaptogenesis. Similarly, recent work on the voltage-gated calcium channel ($Ca_v1.4$) revealed that it has different developmental functions in rod photoreceptor synapses (Maddox et al., 2020). Complete knock-out of the $Ca_v1.4$ channel results in retinal lamination defects and absence of rod photoreceptor synapses (Liu et al., 2013; Zabouri and Haverkamp, 2013; Regus-Leidig et al., 2014). However, a single point mutation in $Ca_v1.4$ that abolishes Ca^{2+} influx leads to a milder phenotype where photoreceptor synapses are still largely formed but they are not functional (Maddox et al., 2020). These data suggest that the calcium channel $Ca_v1.4$ may be required at early stages to structurally recruit key proteins to the synapse and at later stages to mediate functional activity. β II-spectrin may have a similar role where it functions at later developmental stages to recruit specific molecules to aid in synapse formation of the rod pathway.

Taken together, our work in the retina uncovered a new developmental role of β II-spectrin in building neural circuits. The discovery of new molecular pathways could provide insights into mechanisms of assembling neural circuits and how these could lead to aberrant wiring in individuals with neurodevelopmental disorders.

References

- Abd-El-Barr MM, Pennesi ME, Saszik SM, Barrow AJ, Lem J, Bramblett DE, Paul DL, Frishman LJ, Wu SM (2009) Genetic dissection of rod and cone pathways in the dark-adapted mouse retina. *J Neurophysiol* 102:1945–1955.
- Bennett V, Lorenzo DN (2013) Spectrin- and ankyrin-based membrane domains and the evolution of vertebrates. *Curr Top Membr* 72:1–37.
- Bennett V, Lorenzo DN (2016) An adaptable spectrin/ankyrin-based mechanism for long-range organization of plasma membranes in vertebrate tissues. *Curr Top Membr* 77:143–184.
- Bozzi Y, Casarosa S, Caleo M (2012) Epilepsy as a neurodevelopmental disorder. *Front Psychiatry* 3:19.
- Burger CA, Jiang D, Mackin RD, Samuel MA (2021) Development and maintenance of vision's first synapse. *Dev Biol* 476:218–239.
- Cao Y, Sarria I, Fehlhaber KE, Kamasawa N, Orlandi C, James KN, Hazen JL, Gardner MR, Farzan M, Lee A, Baker S, Baldwin K, Sampath AP, Martemyanov KA (2015) Mechanism for selective synaptic wiring of rod photoreceptors into the retinal circuitry and its role in vision. *Neuron* 87:1248–1260.
- Carter-Dawson LD, LaVail MM (1979) Rods and cones in the mouse retina. II. Autoradiographic analysis of cell generation using tritiated thymidine. *J Comp Neurol* 188:263–272.
- Cousin MA, et al. (2021) Pathogenic SPTBN1 variants cause an autosomal dominant neurodevelopmental syndrome. *Nat Genet* 53:1006–1021.
- Dick O, tom Dieck S, Altmann WD, Ammermüller J, Weiler R, Garner CC, Gundelfinger ED, Brandstätter JH (2003) The presynaptic active zone protein bassoon is essential for photoreceptor ribbon synapse formation in the retina. *Neuron* 37:775–786.
- Eshed Y, Feinberg K, Poliak S, Sabanay H, Sarig-Nadir O, Spiegel I, Birmingham JR Jr, Peles E (2005) Gliomedin mediates Schwann cell-axon interaction and the molecular assembly of the nodes of Ranvier. *Neuron* 47:215–229.

- Faux C, Rakic S, Andrews W, Britto JM (2012) Neurons on the move: migration and lamination of cortical interneurons. *Neurosignals* 20:168–189.
- Galiano MR, Jha S, Ho TS, Zhang C, Ogawa Y, Chang KJ, Stankewich MC, Mohler PJ, Rasband MN (2012) A distal axonal cytoskeleton forms an intra-axonal boundary that controls axon initial segment assembly. *Cell* 149:1125–1139.
- Ho TS, Zollinger DR, Chang KJ, Xu M, Cooper EC, Stankewich MC, Bennett V, Rasband MN (2014) A hierarchy of ankyrin-spectrin complexes clusters sodium channels at nodes of Ranvier. *Nat Neurosci* 17:1664–1672.
- Hoon M, Okawa H, Della Santina L, Wong RO (2014) Functional architecture of the retina: development and disease. *Prog Retin Eye Res* 42:44–84.
- Hoon M, Sinha R, Okawa H, Suzuki SC, Hirano AA, Brecha N, Rieke F, Wong RO (2015) Neurotransmission plays contrasting roles in the maturation of inhibitory synapses on axons and dendrites of retinal bipolar cells. *Proc Natl Acad Sci U S A* 112:12840–12845.
- Hyvönen M, Macias MJ, Nilges M, Oschkinat H, Saraste M, Wilmanns M (1995) Structure of the binding site for inositol phosphates in a PH domain. *EMBO J* 14:4676–4685.
- Ikeda Y, Dick KA, Weatherspoon MR, Gincel D, Armbrust KR, Dalton JC, Stevanin G, Dürr A, Zühlke C, Bürk K, Clark HB, Brice A, Rothstein JD, Schut LJ, Day JW, Ranum LP (2006) Spectrin mutations cause spinocerebellar ataxia type 5. *Nat Genet* 38:184–190.
- Lefebvre JL, Zhang Y, Meister M, Wang X, Sanes JR (2008) gamma-Protocadherins regulate neuronal survival but are dispensable for circuit formation in retina. *Development* 135:4141–4151.
- Li S, Chen D, Sauv e Y, McCandless J, Chen YJ, Chen CK (2005) Rhodopsin-Cre transgenic mouse line for Cre-mediated rod-specific gene targeting. *Genesis* 41:73–80.
- Liu X, Kerov V, Haeseleer F, Majumder A, Artemyev N, Baker SA, Lee A (2013) Dysregulation of Ca(v)1.4 channels disrupts the maturation of photoreceptor synaptic ribbons in congenital stationary night blindness type 2. *Channels (Austin)* 7:514–523.
- Lorenzo DN (2020) Cargo hold and delivery: ankyrins, spectrins, and their functional patterning of neurons. *Cytoskeleton (Hoboken)* 77:129–148.
- Lorenzo DN, Badea A, Zhou R, Mohler PJ, Zhuang X, Bennett V (2019) β II-spectrin promotes mouse brain connectivity through stabilizing axonal plasma membranes and enabling axonal organelle transport. *Proc Natl Acad Sci U S A* 116:15686–15695.
- Maddox JW, Randall KL, Yadav RP, Williams B, Hagen J, Derr PJ, Kerov V, Della Santina L, Baker SA, Artemyev N, Hoon M, Lee A (2020) A dual role for Ca_v1.4 Ca²⁺ channels in the molecular and structural organization of the rod photoreceptor synapse. *Elife* 9:e62184.
- Martersteck EM, Hirokawa KE, Evarts M, Bernard A, Duan X, Li Y, Ng L, Oh SW, Ouellette B, Royall JJ, Stoeklin M, Wang Q, Zeng H, Sanes JR, Harris JA (2017) Diverse central projection patterns of retinal ganglion cells. *Cell Rep* 18:2058–2072.
- Moon HM, Wynshaw-Boris A (2013) Cytoskeleton in action: lissencephaly, a neuronal migration disorder. *Wiley Interdiscip Rev Dev Biol* 2:229–245.
- Morgan JL, Dhingra A, Vardi N, Wong RO (2006) Axons and dendrites originate from neuroepithelial-like processes of retinal bipolar cells. *Nat Neurosci* 9:85–92.
- Muresan V, Stankewich MC, Steffen W, Morrow JS, Holzbaur EL, Schnapp BJ (2001) Dynactin-dependent, dynein-driven vesicle transport in the absence of membrane proteins: a role for spectrin and acidic phospholipids. *Mol Cell* 7:173–183.
- Pan YH, Wu N, Yuan XB (2019) Toward a better understanding of neuronal migration deficits in autism spectrum disorders. *Front Cell Dev Biol* 7:205.
- Perkins EM, Clarkson YL, Sabatier N, Longhurst DM, Millward CP, Jack J, Toraiwa J, Watanabe M, Rothstein JD, Lyndon AR, Wyllie DJ, Dutia MB, Jackson M (2010) Loss of beta-III spectrin leads to Purkinje cell dysfunction recapitulating the behavior and neuropathology of spinocerebellar ataxia type 5 in humans. *J Neurosci* 30:4857–4867.
- Pielage J, Fetter RD, Davis GW (2006) A postsynaptic spectrin scaffold defines active zone size, spacing, and efficacy at the *Drosophila* neuromuscular junction. *J Cell Biol* 175:491–503.
- Pourhoseini S, Goswami-Sewell D, Zuniga-Sanchez E (2021) Neurofascin is a novel component of rod photoreceptor synapses in the outer retina. *Front Neural Circuits* 15:635849.
- Rasband MN, Peles E (2021) Mechanisms of node of Ranvier assembly. *Nat Rev Neurosci* 22:7–20.
- Regus-Leidig H, Atorf J, Feigenspan A, Kremers J, Maw MA, Brandst atter JH (2014) Photoreceptor degeneration in two mouse models for congenital stationary night blindness type 2. *PLoS One* 9:e86769.
- Ribic A, Liu X, Crair MC, Biederer T (2014) Structural organization and function of mouse photoreceptor ribbon synapses involve the immunoglobulin protein synaptic cell adhesion molecule 1. *J Comp Neurol* 522:900–920.
- Rowan S, Cepko CL (2004) Genetic analysis of the homeodomain transcription factor Chx10 in the retina using a novel multifunctional BAC transgenic mouse reporter. *Dev Biol* 271:388–402.
- Samuel MA, Voinescu PE, Lilley BN, de Cabo R, Foretz M, Viollet B, Pawlyk B, Sandberg MA, Vavvas DG, Sanes JR (2014) LKB1 and AMPK regulate synaptic remodeling in old age. *Nat Neurosci* 17:1190–1197.
- Sarin S, Zuniga-Sanchez E, Kurmangaliyev YZ, Cousins H, Patel M, Hernandez J, Zhang KX, Samuel MA, Morey M, Sanes JR, Zipursky SL (2018) Role for Wnt signaling in retinal neuropil development: analysis via RNA-seq and in vivo somatic CRISPR mutagenesis. *Neuron* 98:109–126.e8.
- Sato S, Omori Y, Katoh K, Kondo M, Kanagawa M, Miyata K, Funabiki K, Koyasu T, Kajimura N, Miyoshi T, Sawai H, Kobayashi K, Tani A, Toda T, Usukura J, Tano Y, Fujikado T, Furukawa T (2008) Pikachurin, a dystroglycan ligand, is essential for photoreceptor ribbon synapse formation. *Nat Neurosci* 11:923–931.
- Shekhar K, Lapan SW, Whitney IE, Tran NM, Macosko EZ, Kowalczyk M, Adiconis X, Levin JZ, Nemesh J, Goldman M, McCarroll SA, Cepko CL, Regev A, Sanes JR (2016) Comprehensive classification of retinal bipolar neurons by single-cell transcriptomics. *Cell* 166:1308–1323.e30.
- Soto F, Watkins KL, Johnson RE, Schottler F, Kerschensteiner D (2013) NGL-2 regulates pathway-specific neurite growth and lamination, synapse formation, and signal transmission in the retina. *J Neurosci* 33:11949–11959.
- Tang Y, Katuri V, Dillner A, Mishra B, Deng CX, Mishra L (2003) Disruption of transforming growth factor-beta signaling in ELF beta-spectrin-deficient mice. *Science* 299:574–577.
- Tse DY, Lotfi P, Simons DL, Sardiello M, Wu SM (2015) Electrophysiological and histological characterization of rod-cone retinal degeneration and microglia activation in a mouse model of mucopolysaccharidosis type IIIB. *Sci Rep* 5:17143.
- Young RW (1985) Cell differentiation in the retina of the mouse. *Anat Rec* 212:199–205.
- Zabouri N, Haverkamp S (2013) Calcium channel-dependent molecular maturation of photoreceptor synapses. *PLoS One* 8:e63853.
- Zhang C, Kolodkin AL, Wong RO, James RE (2017) Establishing wiring specificity in visual system circuits: from the retina to the brain. *Annu Rev Neurosci* 40:395–424.